

RSC Advances



This is an *Accepted Manuscript*, which has been through the Royal Society of Chemistry peer review process and has been accepted for publication.

Accepted Manuscripts are published online shortly after acceptance, before technical editing, formatting and proof reading. Using this free service, authors can make their results available to the community, in citable form, before we publish the edited article. This *Accepted Manuscript* will be replaced by the edited, formatted and paginated article as soon as this is available.

You can find more information about *Accepted Manuscripts* in the [Information for Authors](#).

Please note that technical editing may introduce minor changes to the text and/or graphics, which may alter content. The journal's standard [Terms & Conditions](#) and the [Ethical guidelines](#) still apply. In no event shall the Royal Society of Chemistry be held responsible for any errors or omissions in this *Accepted Manuscript* or any consequences arising from the use of any information it contains.

**Corrosion resistance and adsorption behavior of
bis-(γ -triethoxysilylpropyl)-tetrasulfide self-assembled membrane on
6061 Aluminum alloy**

Yu-qing Wen^{a,b,*}, Hui-min Meng^a, Wei Shang^b

a Corrosion and Protection Center, Laboratory for Corrosion-Erosion and Surface Technology,

University of Science and Technology Beijing, Beijing 100083, China

b Guangxi Key Laboratory of Electrochemical and Magnetochemical Function Materials, Guilin

University of Technology, Guilin, 541004, China

Abstract:

The bis-(γ -triethoxysilylpropyl)-tetrasulfide (BTESPT) self-assembled membrane (the SAM) was prepared by self-assembled membrane technology on 6061 aluminum alloy. The SAM was evaluated using electrochemical techniques (potentiodynamic polarization and electrochemical impedance) in 3.5wt. % NaCl solution. Another, the molecular dynamics calculations showed that the high binding energy between the self-assembled molecule and aluminum alloy surface. The formation of the self-assembled molecule was believed to be achieved by the chemical bond between the silicon oxide group and the metal surface atoms. And last, X-ray photoelectron

spectroscopy and scanning electron microscopy were carried out to confirm the BTESPT could form membrane on 6061 aluminum alloy.

Keywords: Aluminum Alloy; the Self-Assembled Membrane; Corrosion Resistance; Molecular Dynamics Calculations.

1 Introduction

Aluminum alloy have many advantages, such as small density, good ductility, high strength, good electrical conductivity, easy processing, etc., and have been widely used in many fields such as electronic, aerospace, national defense and so on. However, the surface of the aluminum alloy surface often localized corrosion because of the surface oxide film was destroyed in the medium of corrosive ions. These leads to the reduction of the life of the aluminum alloy component. Nowadays, chromate conversion coating is one of the most used adhesion promoters for aluminum and its alloys due to its characteristics such as easy application and effectiveness ^[1]. Recently, environmental requirements are prompting many surface suppliers to develop new technologies based on environmental friendly processes ^[2]. Therefore, it is significant to study the corrosion inhibition technology of aluminum alloy in corrosive media. The self-assembled membrane technology (self-assembled membrane, SAM) is one of the most effective

methods in improving the corrosion resistance of aluminum alloy. In addition, the SAM technology has the unique advantages of no pollution, low cost, etc.

Nowadays, the self-assembled membrane was used in metal anticorrosion research mainly focused on relatively uniform surface of pure metal aspects e.g. Au, Ag, Cu, Fe, and Al^[3-8], and there were very few reports about the applications of self-assembled membrane on alloy surface^[9-14].

In this work, the SAM of bis-(γ -triethoxysilylpropyl)-tetrasulfide (BTESPT) was prepared by self-assembled (SA) method. Its corrosion resistance was synthesized by electrochemical techniques (potentiodynamic polarization and electrochemical impedance). And the mechanism of the BTESPT self-assembled membranes formation was used to study by using molecular dynamics simulation method^[15, 16]. The results of theoretical calculations were verified by SEM and XPS tests.

2 Experimental details

2.1 Material

The working electrodes (with dimensions 30mm×40 mm×3 mm) were prepared from an Al alloy 6061 sheet with the chemical composition (wt. %) of: Si (0.3), Fe (0.7), Cu (0.25), Mn (1.0–1.5), Mg (0.8–1.3), Zn (0.25) and Al (balance). Before SAM treatment, the working electrodes were successively polished with a series of abrasive papers and degreased in an alkaline solution, then sealed with epoxy resin leaving the polished square surface with an area of 1 cm² and ultrasonically cleaned with anhydrous

ethanol and distilled water. Then the working electrodes was immersed into a freshly prepared bis-(γ -triethoxysilylpropyl)-tetrasulfide (BTESPT) mixed solution with methanol and distilled water (3 h), Followed by ultra-pure water to remove the rest of the BTESPT solution (2 min), Finally dried in 100 °C air.

2.2 Measure methods

The surface morphology of the SAM was observed with a JSM-6360LV scanning electron microscopy (SEM). All electrochemical experiments were performed using an electrochemical workstation (CHI660C, Shanghai Chenhua Co., China). A three-electrode cell was used for the electrochemical measurements. The working electrode was SAM modified Al sheet, the counter and the reference electrodes were a large platinum foil (about 3 cm²) and a saturated calomel electrode (SCE), respectively. A 3.5 wt. % NaCl solution was used as the electrolyte. Dynamic measurements of polarization curves were acquired at a scan rate of 0.5 mV/s in Tafel model when the open circuit potential (OCP) became stable. The corrosion current (i_{corr}) and corrosion potential (E_{corr}) were obtained automatically from the Tafel plots using the Electrochemical Workstation analysis software. EIS measurement was operated in the frequency range of 10⁵–10⁻² Hz at the OCP. The ac signal amplitude was 10 mV. The corrosion resistance of the SAM sample was compared with the bare aluminum alloy substrate.

2.3 Molecular dynamics calculation details

The Discover molecular dynamics module in Materials Studio 6.0 software from Accelrys Inc ^[17] allows to select a thermodynamic ensemble and the associated parameters, defining simulation time, temperature and pressuring and initiating a dynamics calculation. The molecular dynamics simulation procedures have been described elsewhere ^[18]. The first step to calculate the interaction energy between the self-assembled molecule and the metal surface was to build the aluminum (1 1 0) surface by importing the aluminum crystal and then cleave its surface through the cleavage plane (1 1 0). To get an accurate result, the thickness of the surface must be more than the non-bond cut-off distances in the force field. After building the aluminum (1 1 0) surface, the surface must be relaxed by minimizing its energy using molecular mechanics. The next step was to increase the surface area of the aluminum (1 1 0) and changing its periodicity by constructing a super cell and building a vacuum slab with zero thickness. The BTESPT was built using the sketching tools in Materials Visualizer and their geometries were optimized. In the third step, the supercell which contains 400 water molecules and BTESPT molecule were created with size of 40.49Å, 28.63Å, 11.50Å. Subsequent, another supercell which contains 200 water molecules were created with size of 40.49Å, 28.63Å, 7.73Å. Finally, all atoms were fixed in the process of simulation layers, the entire model size was 40.49Å, 28.63Å, 36.25Å (Fig 1). The

whole system was performed at 298 K controlled by the Andersen thermostat, NVT ensemble, with a time step of 1.0 fs and simulation time of 500ps, using the COMPASS force field. The MD simulation was carried out in a simulation box (40.49Å×28.63Å×36.25Å) with periodic boundary conditions. The box included Al slab, a self-assembled molecule solution layer.

The interaction energy E_{Al-SAM} of the Al surface with the BTESPT was calculated according to the following equation $E_q(1)$:

$$E_{Al-SAM} = E_{complex} - (E_{Al} + E_{SAM}) \quad E_q(1)$$

where $E_{complex}$ is the total energy of the Al crystal together with the adsorbed self-assembly molecular, E_{Al} and E_{SAM} are the total energy of the Al crystal and free self-assembly molecular, respectively. The binding energy of the inhibitor molecule is the negative value of the interaction energy $E_q(2)$ ^[19].

$$E_{binding} = E_{Al-SAM} \quad E_q(2)$$

3 Results and discussion

3.1 Potentiodynamic polarization curves

The polarization curves of the BTESPT SAM and aluminum alloy matrix in a 3.5 wt. % NaCl solution were showed in Fig. 2. The samples with the SAM showed higher corrosion resistance than the bare aluminum alloy in Fig.2. The parameters of the pitting corrosion potential (E_{pit}) and corrosion potential (E_{corr}), corrosion current density (i_{corr}),

anodic/cathode Tafel constant (β_a and β_c) were derived directly from the polarization curves by Tafel region extrapolation. The corrosion resistance (R_p) was calculated on the basis of the following $E_q(3)$ [20].

$$R_p = \frac{\beta_a \beta_c}{2.3 i_{corr} (\beta_a + \beta_c)} \quad E_q(3)$$

The results were summarized in Table 1. As shown in Fig. 2 and Table 1, the SAM on aluminum alloy obviously reduced i_{corr} and caused the E_{corr} and E_{pit} shift (about 0.3316V). The corrosion potential shifted positively contributes to increase the difficulty of metal corrosion. The higher E_{pit} was considered to be affected by the denser and less pitting surface. The lower i_{corr} and higher R_p mean that the SAM could effectively block aluminum alloy from the anodic dissolution of Al^{+3} . And from the Fig 1, it was showed that the effect of the membranes on the anodic reaction was more observable than that on the cathode reaction. These means that the SAM act as a mixed type of inhibitor.

3.2 Electrochemical impedance spectroscopy (EIS)

The electrochemical impedance spectroscopy (EIS) measurements were carried out to estimate healing effect. The results of the EIS measurements were presented in Fig. 3 as Bode plots. Impedance measurements were conducted in 3.5 wt. % NaCl solution. It was clearly showed that the samples with the SAM had higher impedance value than bare Al alloy in Fig. 3. The impedance of the bare Al alloy was in the range of 10^3

$\Omega\cdot\text{cm}^2$ at low frequencies. In the same frequency range, the impedance of the SAM was increased to the range of $10^5 \Omega\cdot\text{cm}^2$, increased by two order of magnitude. It was indicated that the SAM was an effective membrane formed on aluminum alloy. It could be inferred that the membrane that acts as a blocking barrier for chloride ions attracting the surface.

3.3 Scanning electron microscopy

To establish whether inhibition was due to the formation of the self-assembled membrane on the 6061 aluminum alloy surface via adsorption scanning electron photograph were taken (Fig. 4). The Fig. 4A showed that the surface of the 6061 aluminum alloy. Polishing scratches were also visible. The morphology of the BTESPT self-assembled membrane surface in Fig. 4B. It could be clearly seen that the self-assembled membrane of network covered the surface of Al alloy comparing with the aluminum alloy substrate. And the BTESPT self-assembled membrane was compact. It could infer that the special network structure was conducive to the protection of the Al alloy. It could be verified from the electrochemical performance test results. So, the SAM could had better corrosion resistance than the aluminum alloy substrate in the air.

3.4 Molecular dynamics calculations

The molecular dynamic simulations was performed to study the BTESPT self-assembled behavior on the Al (1 1 0) surface. In this simulation, Al (1 1 0) surface

was chosen among the three kinds of Al surfaces (1 1 0, 1 0 0, 1 1 1), because Al (1 1 0) surface was the most active form ^[21]. According to the above calculation details. It is usually considered that the system reached equilibrium when the temperature and energy were reached balance. The geometry optimization of the studied system was carried out using an iterative process, in which the atomic coordinates were adjusted until the total energy of a structure was minimized. Fig.5 showed the temperature fluctuation curves. Fig.6 showed the energy fluctuation curves. They could be seen that the system tends to equilibrium by the end of the simulation process in Fig. 5 and Fig. 6. And the calculated value of $E_{binding}$ according to E_q (4) was 564.21 kJ/mol. The large negative value could be attributed to the strong adsorption between BTESPT molecules and the aluminum alloy surface.

$$E_{binding} = -E_{adsorption} = E_{total} - (E_{surface+solution} + E_{SAM+solution}) + E_{solution} \quad E_q (4)$$

Where E_{total} was the total potential energy of the system; $E_{surface+solution}$ and $E_{SAM+solution}$ were the potential energies of the system without the SAM and the system without the aluminum alloy surface, respectively; $E_{solution}$ was the potential energy of all the water molecules.

The balance graph of the system in the before and after calculation was shown in Fig.7. The organic molecule was surrounded by water, and only the four S atoms were closest to the aluminum alloy surface in Fig. 7A. While two silicon oxygen groups were far from the metal surface. (Fig. 7A). When the calculation was over, the two silicon

oxygen groups closed to the aluminum alloy surface atoms, even closer to the metal surface than the four S atoms (Fig. 7B). It could be deduced that the formation of the self-assembled membrane was mainly dependent on interaction between the silicon oxygen groups and the metal surface atoms by the comparison of the model before and after the dynamics simulation. The role of the self-assembled membrane was a barrier to corrosion medium between the corrosive medium and the metal surface.

The radial distribution function, (or pair correlation function) $g(r)$ in a system of particles (atoms, molecules, colloids, etc.), describes how density varies as a function of distance from a reference particle. It is a characteristic physical quantity which reflects the microstructure of the material. The radial distribution function can provide information of the degree of order of the simulation system^[22]. When appear greater than 3 Å peak, it indicates that the molecular chain of long-range order belong to the crystallization system. When less than 0.3 Å peak, it indicates that the molecular chain of short-range disorder belong to the amorphous structure. The relative correlation function could be obtained by analyzing the trajectory file of the dynamics simulation. It also analyzed the radial distribution function of the atomic and metal surface atoms in the computational system (Fig. 8). It is generally thought that the formation of a chemical bond in less than 3.5 Å peak, more than 3.5 Å peak is the scope of van der Waals force or Coulomb force in the radial distribution function curve^[23]. From Fig. 8, it was clear that first peaks of S 3.42 Å (Fig. 8B), O 2.97 Å (Fig. 8C) and H 2.99 Å (Fig.

8D) appeared in less than 3.5 Å in radial distribution curve. These results indicated that BTESPT was adsorbed on the aluminum alloy surfaces depends on the interaction between S, O and H and the metal surface atoms. It could be deduced that this was van der Waals force or Coulomb force between C, Si and metal surface atoms, because their first peaks of the atomic radial distribution function were greater than 3.5 Å (C(3.79 Å) Fig. 8E and Si (3.99 Å) Fig. 8F). So, it was inferred that the formation of the BTESPT self-assembled membrane depended mainly on the chemical adsorption of S and O with the metal surface atoms on the 6061 aluminum alloy.

3.5 X-ray photoelectron spectroscopy (XPS)

The XPS measurements were performed to investigate the composition of the self-assembled membrane formed on the 6061 aluminum alloy surface in order to verify the results of the dynamic calculation. It displayed five main elements of C, O, Si, S and Al (Fig. 9). The peaks of Al appeared, which indicated the thickness of the SAM may be beyond the detection depth of XPS. Another, the elements of C, O, and S were main composition in SAM. The C 1s core-level XPS spectra were convoluted into the following four types of carbon bands: 284.82 eV (C-C), 286.48 eV (C-O), 288.78 eV (C=O), and 163.7 eV (S-C) (Fig. 10A, 10C). The Si 2p and O 1s peaks were relatively simple, respectively bands were 102.47 eV and 532.14 eV (Fig. 10B, 10D). It could be

determined that the self-assembled membranes were successfully prepared on the surface of aluminum alloy. The results were in agreement with theoretical calculations.

4 Conclusions

In this study, the BTESPT was investigated as a self-assembled membrane for 6061 aluminum alloy in 3.5 wt. % NaCl solution medium by electrochemical tests, SEM, XPS, and dynamic simulation was used to study the mechanism of the BTESPT self-assembled membrane. The results obtained lead to the following conclusions:

(1) The potentiodynamic polarization study showed that the BTESPT was a mixed type inhibitors by forming the self-assembled membrane on aluminum alloy. And the current density values of BTESPT SAMs working electrode was two orders of magnitude smaller than that of the blank aluminum alloy electrodes, and reached to $8.764 \times 10^{-8} \text{ A} \cdot \text{cm}^2$. And the corrosion resistance of SAM was more 70 times larger than the aluminum alloy blank electrode. Another, the samples with the SAM showed higher impedance value than bare Al alloy by EIS. It was indicated that the SAM was an effective membrane formed on aluminum alloy. So it may be explained that the membrane that acts as a blocking barrier for chloride ions attracting the surface.

(2) The theoretical study of the dynamic simulation indicated that the BTESPT SAM could be adsorbed on aluminum alloy surface by chemisorption, and the binding

energies of BTESPT were 564.21 kJ/mol. The radial distribution function analysis of dynamic simulation confirmed that the formation of the BTESPT self-assembled membrane depended mainly on the chemical adsorption of S and O with the metal surface atoms on the aluminum alloy. The results of theoretical calculations were verified by SEM and XPS tests. The corrosion resistance of the self-assembled membrane was mainly dependent on the interaction between the silicon oxygen functional group and the aluminum alloy surface.

Acknowledgment

This work was financially supported by the Project of Guangxi Natural Science Foundation of China (No. 2014GXNSFAA118335)

References

- [1] P. Santa Coloma, U. Izagirre, Y. Belaustegi, J.B. Jorcin, F.J. Cano, N. Lapeña, *Appl. Surf. Sci.*, 2013, 218, 99-107.
- [2] Hugo C. Novais, Diana M. Fernandes, Cristina Freire, *Appl. Surf. Sci.*, 2015, 347, 40-47.
- [3] Yu. Fei, Shougang Chen, Houmin Li, Lejiao Yang, Yansheng Yin, *Thin Solid Films*, 2012, 520, 4990-4995.

- [4] Shiheng Yin, Wu. Dongxiao, Ji Yang, Shumei Lei, Tongchun Kuang, Bin Zhu, Appl. Surf. Sci., 2011, 257, 8481-8485.
- [5] Mei-Yun Duan, Ren Liang, Na Tian, Yong-Jun Li, Edward S. Yeung, Electrochim. Acta, 2013, 87, 432-437.
- [6] Chia-Jun Wu, Chih-Yuan Lin, Pei-Chi Cheng, Chun-Wei Yeh, Jhy-Der Chen, Ju-Chun Wang. Polyhedron, 2011, 30, 2260-2267.
- [7] Imran Shakir, Zahid Ali, Dae Joon Kang. J. Alloys Compd., 2014, 617, 707-712.
- [8] Thanh Hai Phan, Tomaz Kosmala, Klaus Wandelt, Surf. Sci., 2015, 631, 207-212.
- [9] Feifei Xiang, Chao Li, Zhongping Wang, Xiaoqing Liu, Danfeng Jiang, Xinli Leng, Jie Ling, Li Wang, Surf. Sci., 2015, 633, 46-52.
- [10] A. Venugopal, Rajiv Panda, Sushant Manwatkar, K. Sreekumar, L. Rama Krishna, G. Sundararajan, T. Nonferr. Metal. Soc., 2012, 22, 700-710.
- [11] Yujiang Zhuo, Wendong Sun, Lihong Dong, Ying Chu, Appl. Surf. Sci., 2011, 257, 10395-10401.
- [12] Chao Kang, Houfang Lu, Shaojun Yuan, Dongyin Hong, Kangping Yan, Bin Liang, Chem. Eng. J., 2012, 203, 1-8.
- [13] Viviane Dalmoro, João H.Z. dos Santos, Elaine Armelin, Carlos Alemán, Denise S. Azambuja, Appl. Surf. Sci., 2013, 273, 758-768.
- [14] Dalei Song, Xiaoyan Jing, Jun Wang, Piaoping Yang, Yanli Wang, Milin Zhang, J. Alloys Compd., 2012, 510, 66-70.

- [15] M Lagrenée, B Mernari, N Chaibi, M Traisnel, H Vezin, F Bentiss, *Corros. Sci.*, 2001, 43, 951-962.
- [16] F. Bentiss, M. Traisnel, H. Vezin, M. Lagrenée, *Corros. Sci.*, 2011, 53, 487-495.
- [17] I.B. Obot, Z.M. Gasem, *Corros. Sci.*, 2014, 83, 359-366.
- [18] M. M Kabanda, I.B. Obot, E.E Ebenso, *Int. J. Electrochem. Sci.*, 2013, 8, 10839-10850.
- [19] Baoyu Liu, Hongxia Xi, Zhong Li, Qibin Xia, *Appl. Surf. Sci.*, 2012, 258, 6679-6687.
- [20] Yu-qing Wen, Hui-min Meng, Wei Shang, *Surf. Coat. Technol.*, 2014, 258, 574-579.
- [21] ZHANG Xin-ming, LIU Jian-cai, TANG Jian-guo, CHEN Ming-an, *The Chinese Journal of Nonferrous Metals*, 2009, 19, 1759-1764.
- [22] Angelika Kühnle. *Current Opinion in Colloid & Interface Science*, 2009, 14, 157-168.
- [23] Zhe Zhang, Ningchen Tian, Lingzhi Zhang, Ling Wu. *Corrosion Science*, 2015, 98, 438-449.

List of the figures and table:

Fig.1 The adsorption model of the BTESPT in solution.

Fig.2 Potentiodynamic polarization curves of samples in 3.5% NaCl solutions

Fig.3 Impedance plots of samples in 3.5% wt. NaCl solution

Fig.4 Surface morphology of the aluminum substrate (A) and the SAMs on aluminum alloy 6061 (B).

Fig.5 Temperature equilibrium curve of BTESPT adsorbed on Al (1 1 0) surface

Fig.6 Energy equilibrium curve of BTESPT adsorbed on Al (1 1 0) surface

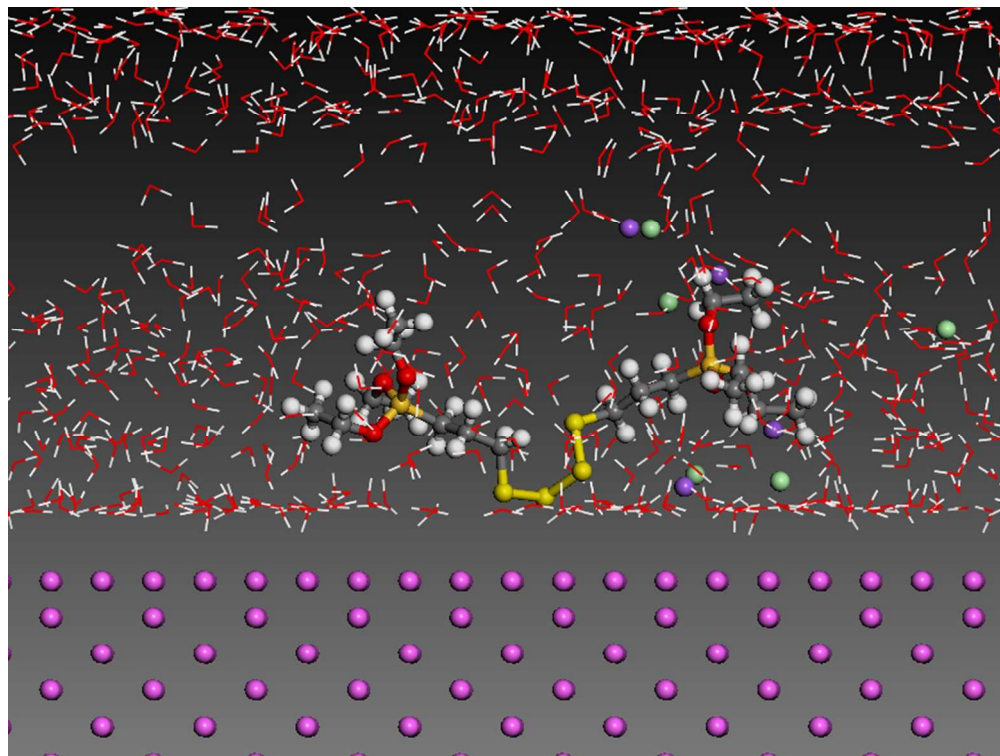
Fig.7 The comparison of configuration with the initial(A) and the final(B) adsorption model on Al (1 1 0) surface

Fig.8 The pair correlation function of Sulphur(B), oxygen(C), hydrogen(D), carbon(E) and silicon(F) atoms from BTESPT with Al atoms from Al (1 1 0) surface in solution

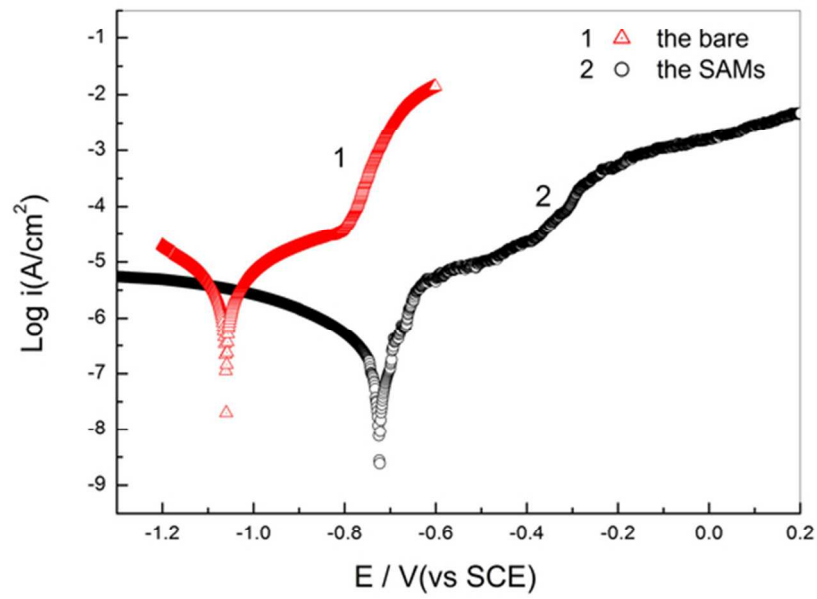
Fig.9 XPS spectra for SAMs of BTESPT

Fig.10 High resolution XPS spectra of the atoms Si(A), O(B), C(C) and S(D)

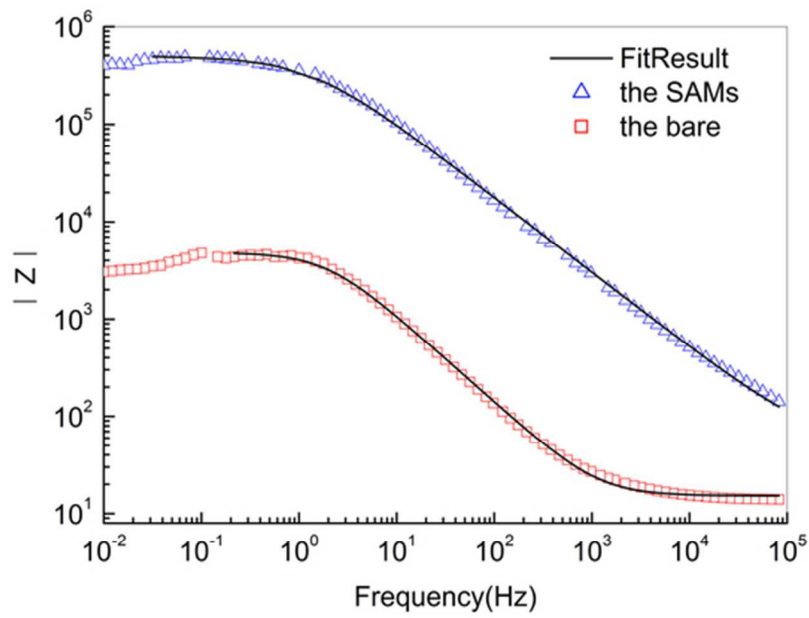
Table.1 Results of potentiodynamic polarization tests of two samples in 3.5-wt. % NaCl solution



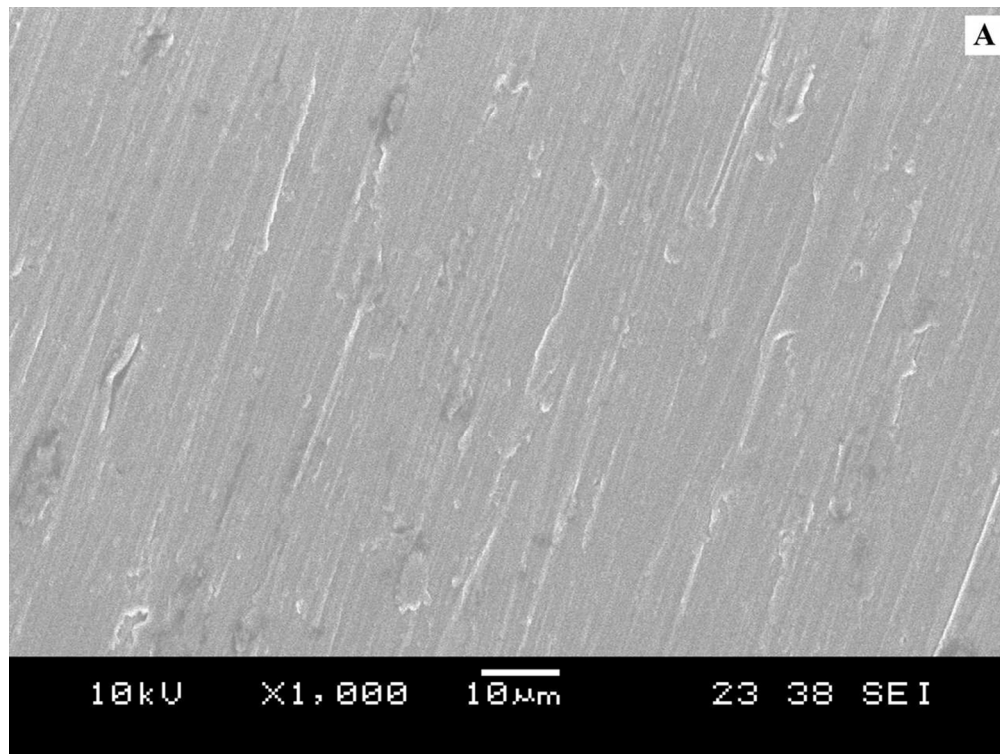
190x142mm (300 x 300 DPI)



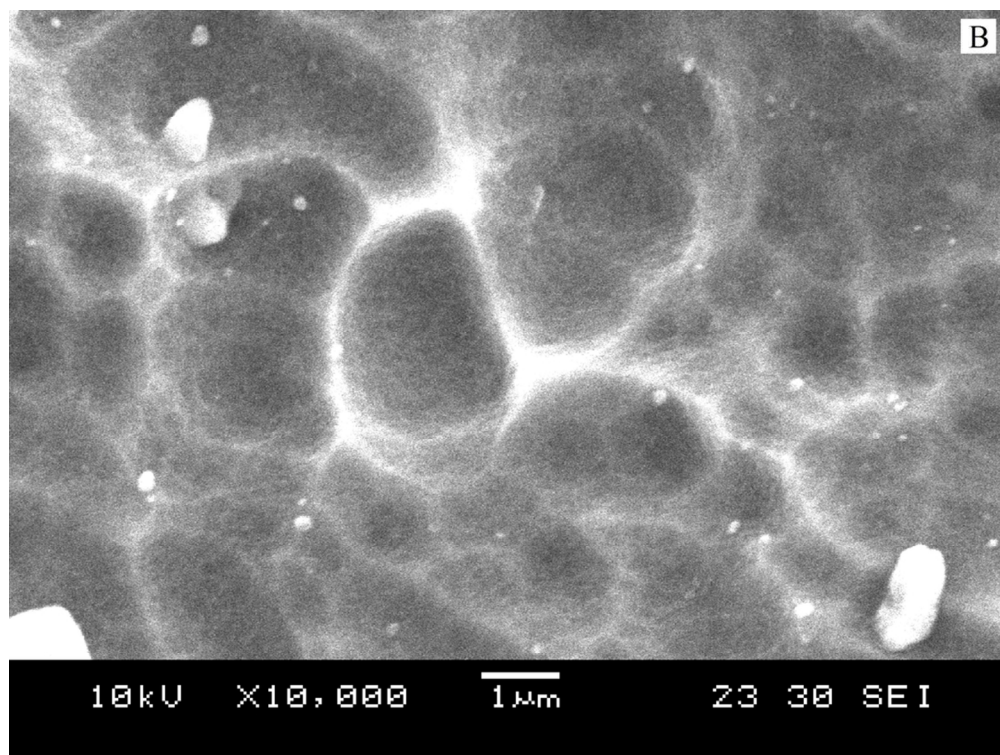
57x40mm (300 x 300 DPI)



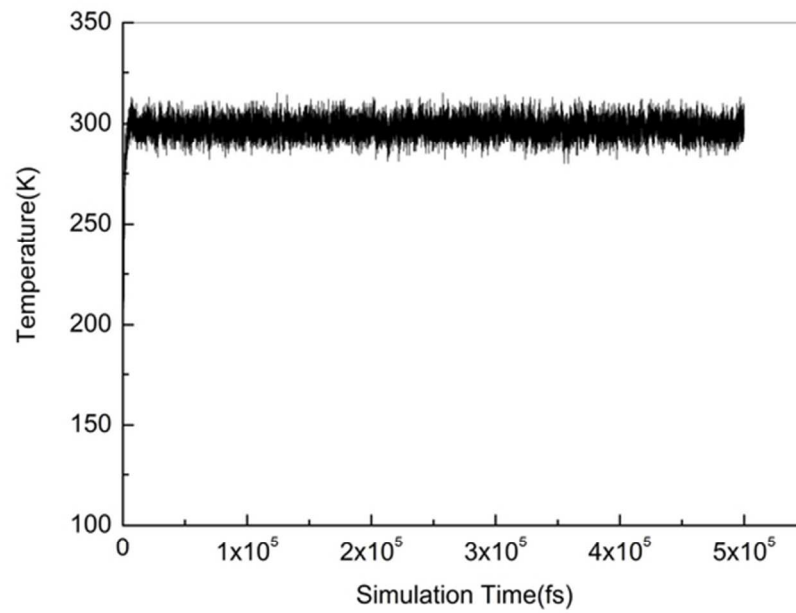
56x39mm (300 x 300 DPI)



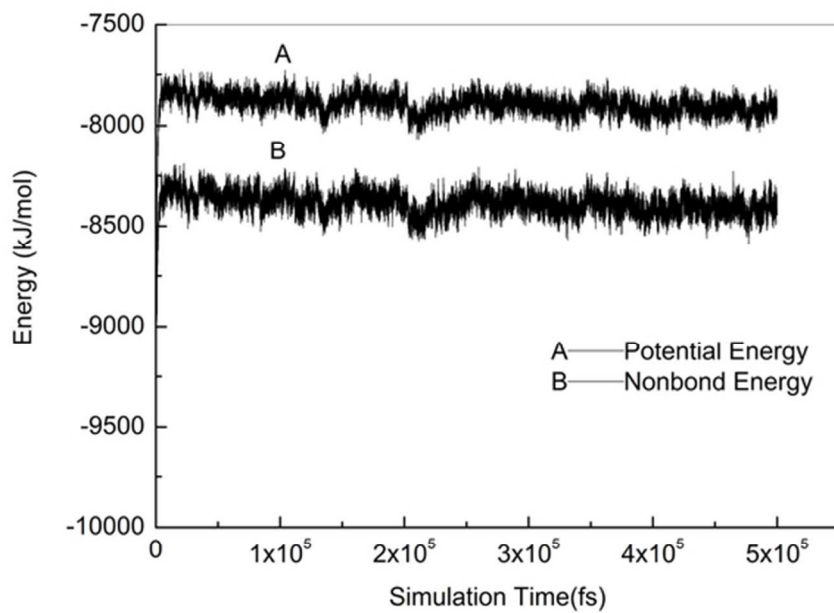
96x72mm (300 x 300 DPI)



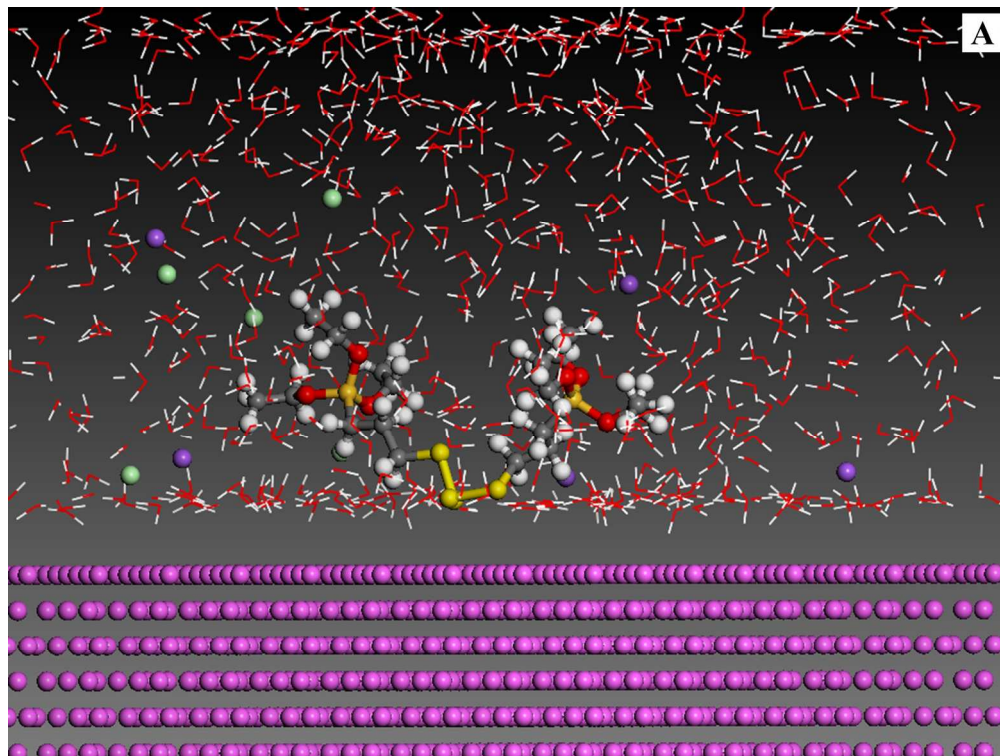
96x72mm (300 x 300 DPI)



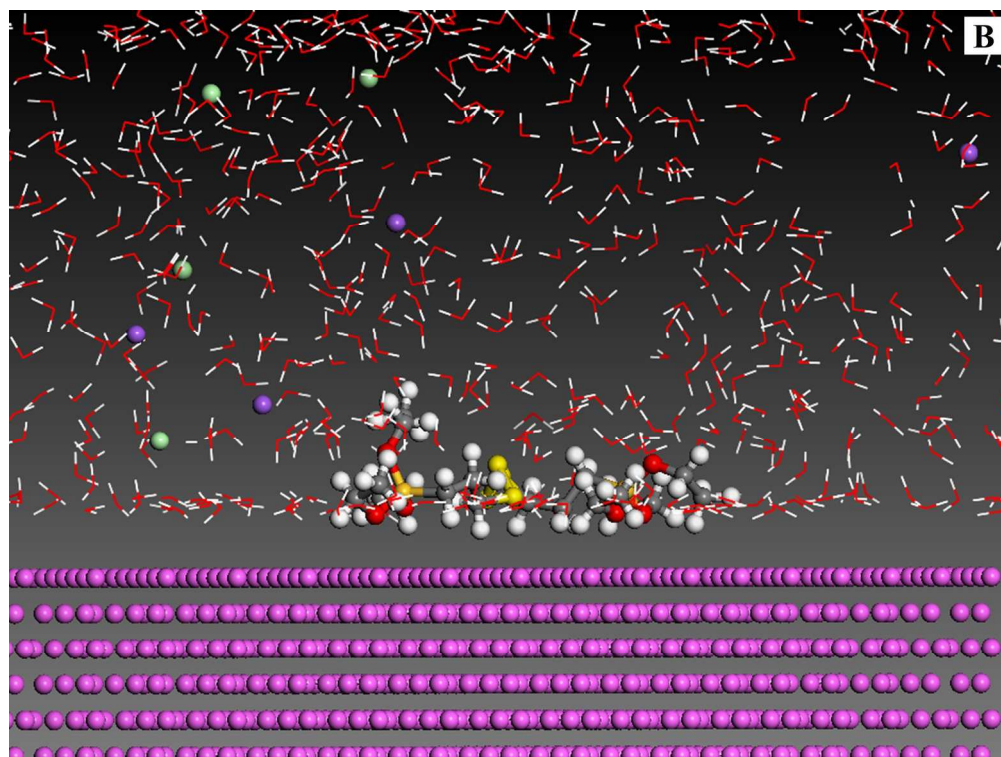
57x40mm (300 x 300 DPI)



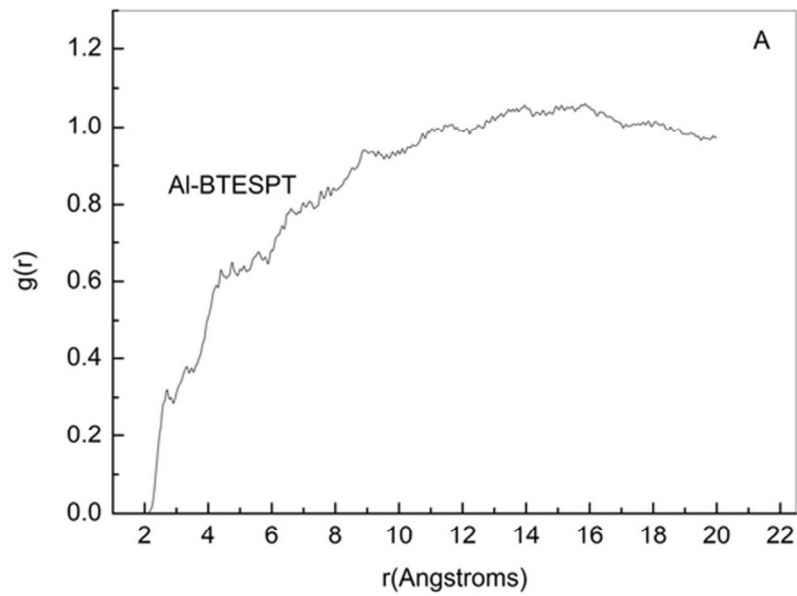
57x40mm (300 x 300 DPI)



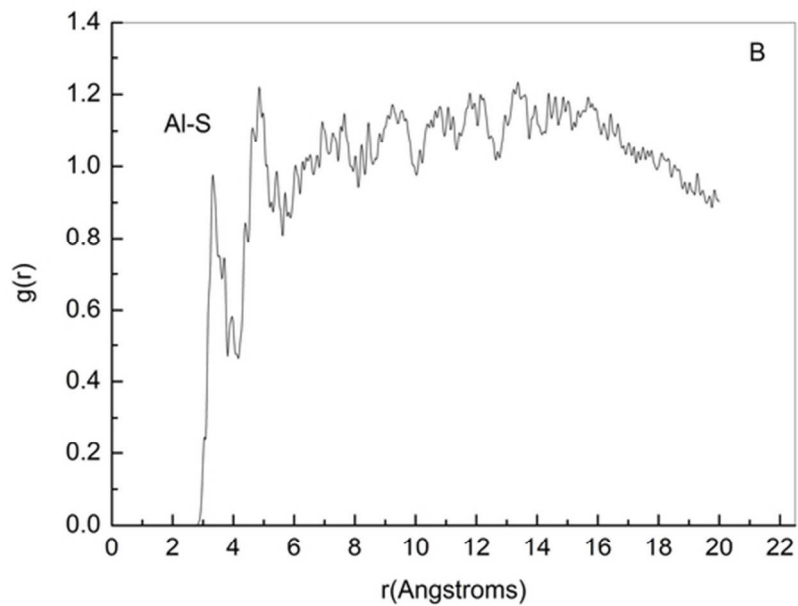
190x142mm (300 x 300 DPI)



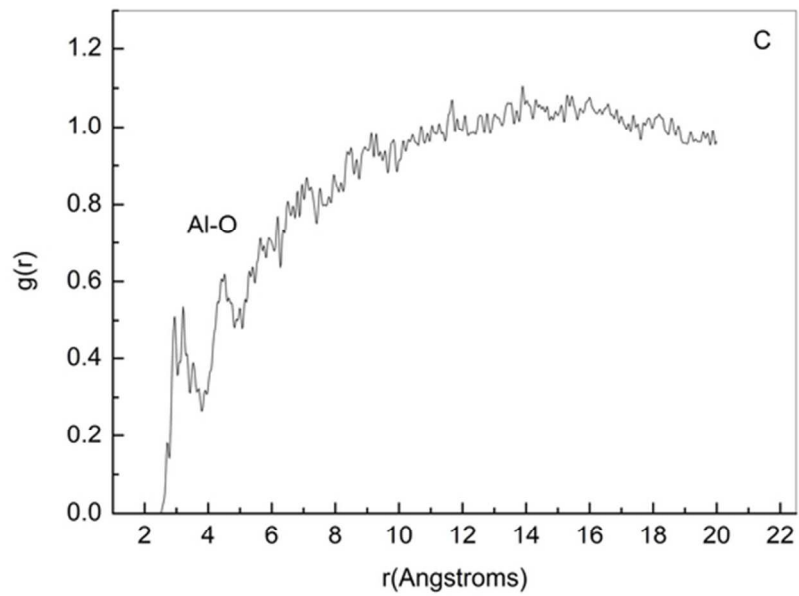
190x142mm (300 x 300 DPI)



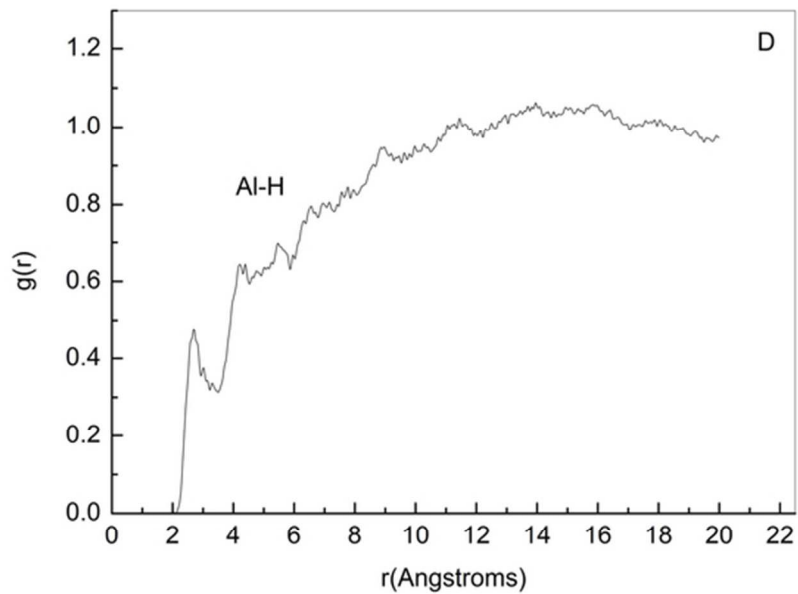
57x40mm (300 x 300 DPI)



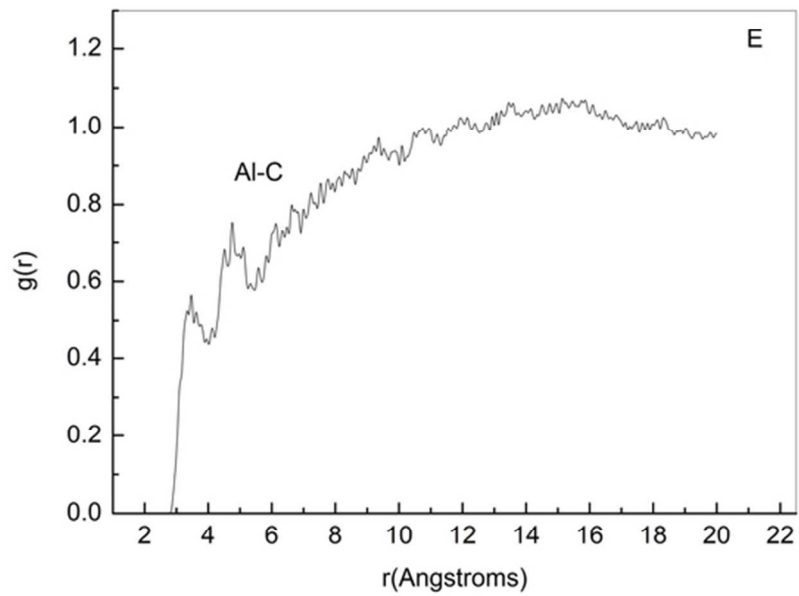
57x40mm (300 x 300 DPI)



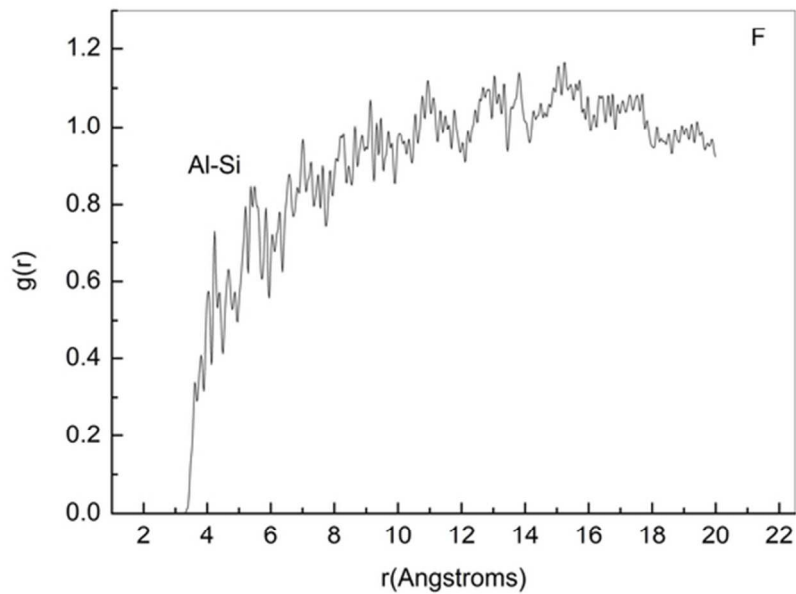
57x40mm (300 x 300 DPI)



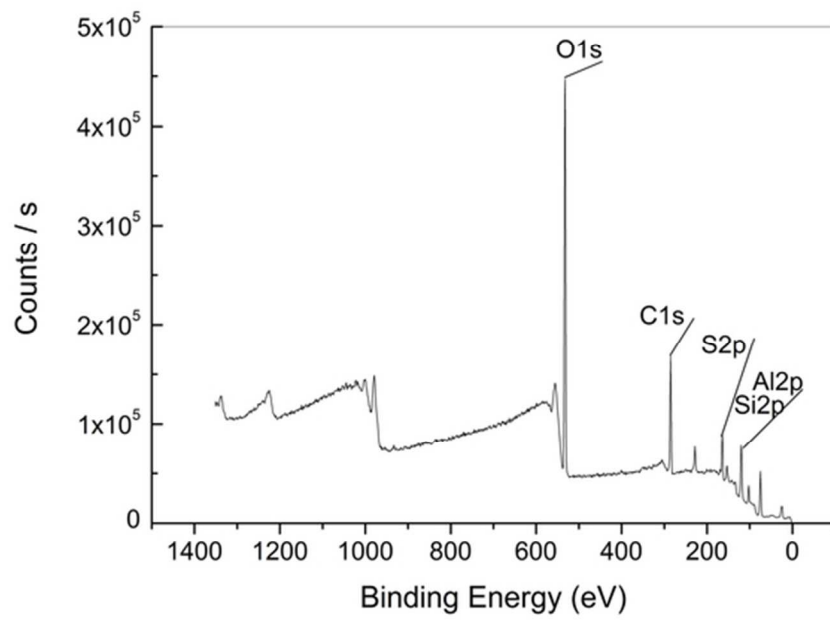
57x40mm (300 x 300 DPI)



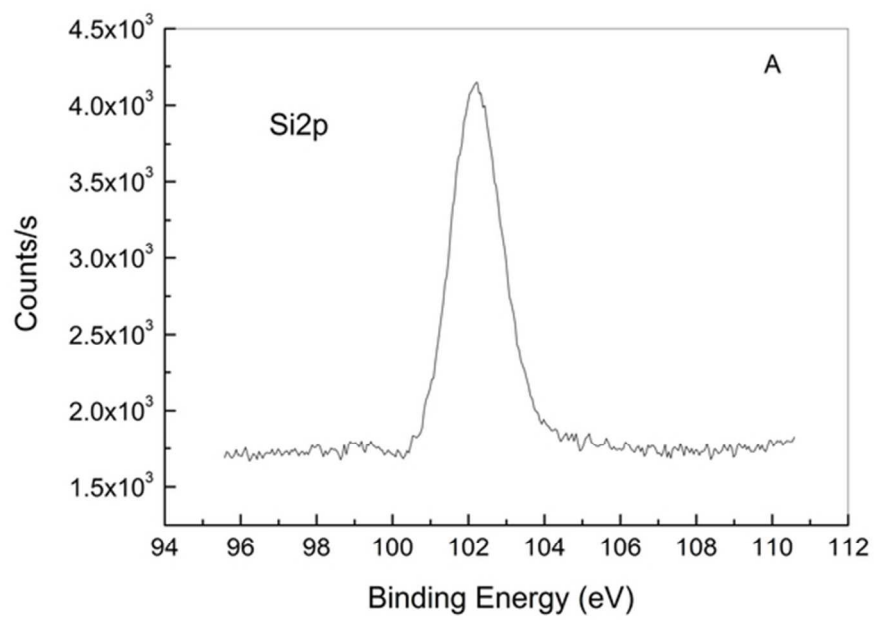
57x40mm (300 x 300 DPI)



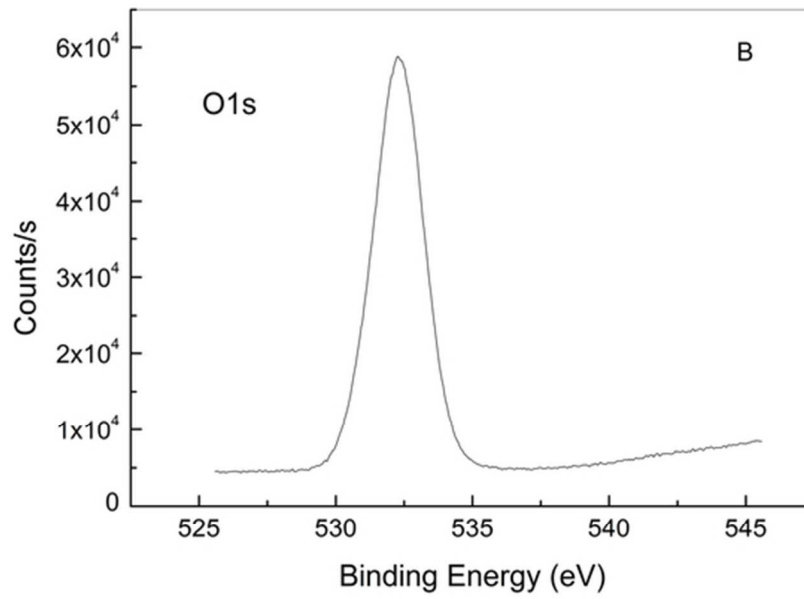
57x40mm (300 x 300 DPI)



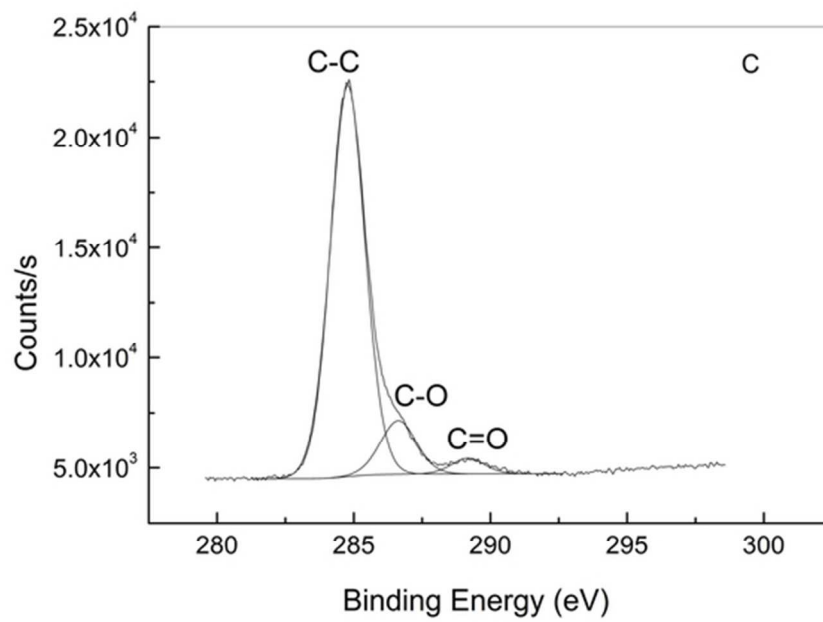
56x39mm (300 x 300 DPI)



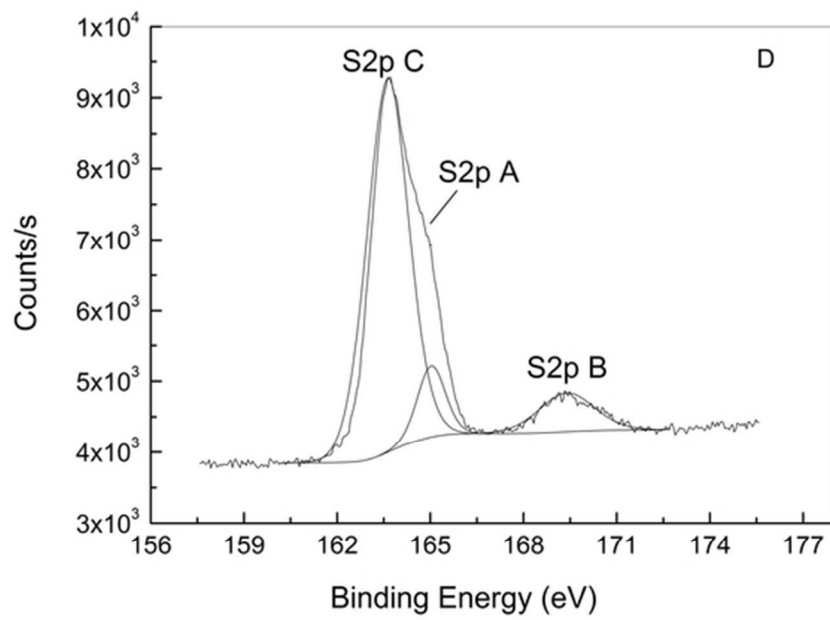
56x39mm (300 x 300 DPI)



56x39mm (300 x 300 DPI)



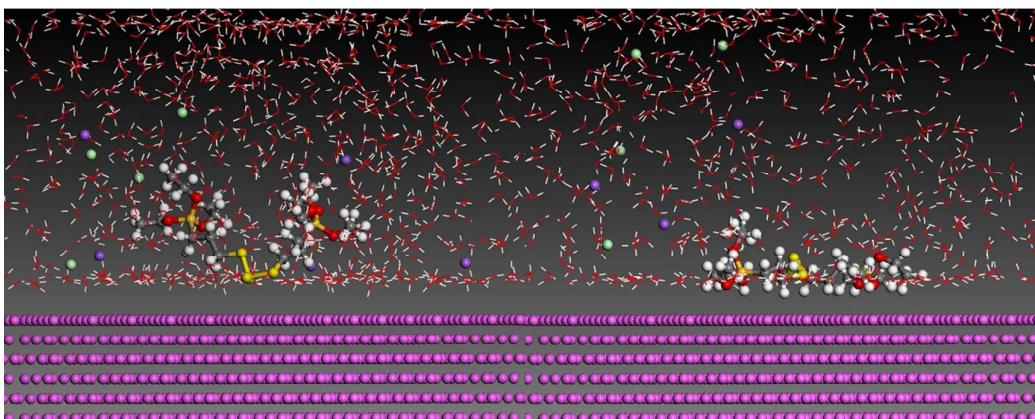
56x39mm (300 x 300 DPI)



56x39mm (300 x 300 DPI)

sample	E_{corr} /V(vs SCE)	E_{pit} /V(vs SCE)	$E_{pit} - E_{corr}$ /V(vs SCE)	β_a /V·decade ⁻¹	β_c /V·decade ⁻¹	i_{corr} /A·cm ⁻²	R_p / Ω
The bare Al alloy	-1.0609	-0.8201	0.2408	0.00524	0.005468	4.806×10^{-6}	242.07
The SAM	-0.7293	-0.3987	0.3306	0.020511	0.004374	8.764×10^{-8}	17885.36

195x43mm (150 x 150 DPI)



The graph was the model before (left) and after (right) the dynamics simulation. It could be deduced that the formation of the self-assembled membrane was mainly dependent on interaction between the silicon oxygen bond and the metal surface atom.